Pair counting, pion-exchange forces and the structure of light nuclei

R. B. Wiringa*
Physics Division, Argonne National Laboratory, Argonne, Illinois 60439, USA
(Received 6 January 2006; published 27 March 2006)

A simple but useful guide for understanding the structure of light nuclei is presented. It is based on counting the number of interacting pairs in different spin-isospin (S, T) states for a given spatial symmetry and estimating the overall binding according to the sum of $\sigma_i \cdot \sigma_j \tau_i \cdot \tau_j$ expectation values, as suggested by one-pion exchange. Applied to s- and p-shell nuclei, this simple picture accounts for the relative stability of nuclei as A increases and as T changes across isobars, the saturation of nuclear binding in the p shell, and the tendency to form d, t, or α subclusters there. With allowance for pairwise tensor and spin-orbit forces, which are also generated or boosted by pion exchange, the model explains why mixing of different spatial symmetries in ground states increases as T increases across isobars and why, for states of the same spatial symmetry, the ones with greater S are lower in the spectrum. The ordering of some sd-shell intruder levels can also be understood. The success of this simple model supports the idea that one-pion exchange is the dominant force controlling the structure of light nuclei.

DOI: 10.1103/PhysRevC.73.034317 PACS number(s): 21.10.−k, 21.45.+v, 21.60.−n

I. INTRODUCTION

The past decade has seen significant progress in both the characterization of realistic two- and three-nucleon interactions, and in the ability to make accurate many-body calculations with these models. Nucleon-nucleon potentials such as Argonne v_{18} [1], CD-Bonn [2,3], and the Nijmegen models [4] reproduce NN scattering data extremely well; when combined with three-nucleon forces such as the Illinois or Tucson-Melbourne potentials [5,6] and accurate many-body techniques, nuclear binding energies up to $A = 12$ can be reproduced. Seven different many-body methods are in superb agreement for the binding energy of ^{4}He with a realistic NN force [7], while Green's function Monte Carlo (GFMC) [8–11], no-core shell model (NCSM) [12–14], and coupled-cluster methods (CCMs) [15,16] are making very successful *ab initio* calculations for p-shell nuclei. This progress allows us to study the interplay between nuclear forces and nuclear structure in an unprecedented manner.

In a recent letter [17] the authors constructed a series of increasingly realistic force models and used GFMC calculations to evaluate the consequences for nuclear structure. This study showed that a simple central potential, with the canonical intermediate-range attraction and short-range repulsion indicated by S-wave NN phase shifts, could approximately reproduce the triton and α binding energies, but failed to saturate in the p shell, producing stable ^{5}He and greatly overbinding the $A = 6$, 7, 8 nuclei. To obtain unstable ^{5}He and the general saturation of nuclear forces that is evident in the p shell, it is necessary to have a state-dependent force, i.e., one that is attractive in $L =$ even partial waves and repulsive in $L =$ odd partial waves. Indeed, state dependence appears to be more important for nuclear saturation than either the repulsive core or the finite range of nuclear forces. To obtain the further refinement that ^{8}Be is unstable against breakup into two α's requires the addition of a tensor force, while the stability of ^{6,7}Li suggests spin-orbit terms are also needed. Together, these are the major operator components required in a realistic interaction for fitting S- and P-wave NN data.

Pion-exchange forces play a very significant role here. The spin-isospin dependence of one-pion exchange (OPE) makes it attractive in $L =$ even partial waves and repulsive in $L =$ odd partial waves, just as required for binding the s-shell nuclei and for the binding to saturate quickly in the p shell. OPE also is the major source of the tensor force, and iterated tensor interactions among three or more nucleons provide a large enhancement to spin-orbit splitting in nuclei [18]. In GFMC calculations of $A \leqslant 12$ nuclei with realistic interactions, the expectation value of the OPE potential is typically 70%–75% of the total potential energy [8]. The importance of pion-exchange forces is even greater when one considers that much of the intermediate-range attraction in the NN interaction can be attributed to uncorrelated two-pion exchange with the excitation of intermediate $\Delta(1232)$ resonances [19]. In addition, two-pion exchange among three nucleons is the leading term in $3N$ interactions, which are required for getting the empirical binding in light nuclei [5]. In particular, the $3N$ forces provide the extra binding required for stabilizing the Borromean nuclei ^{6,8}He and ^{9}Be.

The thesis of this paper is that, by counting the number of different spin-isospin (S, T) pairs that occur in a given nuclear state of specific spatial symmetry and multiplying by a numeric strength taken from the OPE operator $\sigma_i \cdot \sigma_j \tau_i \cdot \tau_j$, one obtains a very good measure of the binding energy. This works both for the relative energy between different states in the same nucleus and between different nuclei. The idea is akin to the supermultiplet theory of Eisenbud Wigner [20], which focused on the symmetry aspects of light nuclei, but assumed forces that were primarily central and space exchange in character. The present study benefits from the extensive recent progress in the fully realistic calculations mentioned above. There is also common ground with the recent work by Otsuka and collaborators [21,22] within the framework of traditional shell model that emphasizes the importance of OPE spin-isospin and

*Electronic address: wiringa@anl.gov

tensor interactions in determining how single-particle energy levels shift as shells are filled.

This simple guide, supplemented by our knowledge of tensor, spin-orbit, and Coulomb forces, describes the general structure of light nuclei in considerable detail. The model explains the growing binding as A increases, the saturation of binding going from the s shell to the p shell, the relative stability as T varies across isobars, and the tendency to form d, t, and α subclusters in the light nuclei. It explains why mixing of different spatial symmetries in ground states increases as T increases and why for states of the same spatial symmetry, the ones of higher S are lower in the spectrum. The same logic can also be used to understand the ordering of some sd-shell intruder levels in these nuclei.

II. PAIR COUNTING

The total number of pairs in a nucleus, $P_A = A(A-1)/2$, can be subdivided into pairs of specific spin and isospin $P_A(ST)$, where $S = 0$ or 1 and $T = 0$ or 1. Starting with the square of the expression $\sum_i \tau_i/2 = T_A$, where T_A is the total isospin of the nucleus, and using the projection operators $(1 - \tau_i \cdot \tau_j)/4$ and $(3 + \tau_i \cdot \tau_j)/4$ for $T = 0$ and 1 pairs, respectively, one can show that the total number of such pairs of given isospin in a nucleus depend on only A and T_A [23]:

$$P_A(10) + P_A(00) = \tfrac{1}{8}[A^2 + 2A - 4T_A(T_A+1)], \quad (1)$$

$$P_A(11) + P_A(01) = \tfrac{1}{8}[3A^2 - 6A + 4T_A(T_A+1)]. \quad (2)$$

A similar pair of equations can be obtained for the total number of $S = 0$ or 1 pairs in terms of the total nuclear spin S_A, assuming spin is conserved, i.e., before configuration mixing by tensor forces and correlations. An additional expression can be obtained for the difference $p_{[n]}$ between the number of symmetric (even) and antisymmetric (odd) pairs for a given spatial symmetry state specified by the Young diagram $[n]$:

$$P_A(10) + P_A(01) - P_A(11) - P_A(00) = p_{[n]}. \quad (3)$$

For example a [3] symmetry state has three symmetric pairs, $p_{[3]} = 3$; a [111] state has three antisymmetric pairs, $p_{[111]} = -3$; and a [21] state has one symmetric, one antisymmetric, and one mixed-symmetry pair (which does not contribute here), giving $p_{[21]} = 0$. Together we have four independent relations for four unknowns, which can be rearranged to give

$$P_A(11) = \tfrac{1}{4}\big[2P_A - p_{[n]} - \tfrac{3}{2}A + S_A(S_A+1) + T_A(T_A+1)\big], \quad (4)$$

$$P_A(10) = \tfrac{1}{4}[P_A + p_{[n]} + S_A(S_A+1) - T_A(T_A+1)], \quad (5)$$

$$P_A(01) = \tfrac{1}{4}[P_A + p_{[n]} - S_A(S_A+1) + T_A(T_A+1)], \quad (6)$$

$$P_A(00) = \tfrac{1}{4}\big[-p_{[n]} + \tfrac{3}{2}A - S_A(S_A+1) - T_A(T_A+1)\big]. \quad (7)$$

One obtains the simple energy measure being proposed for use by multiplying the number of pairs of each type with the expectation value of the spin-isospin operator $\sigma_i \cdot \sigma_j \tau_i \cdot \tau_j$ coming from OPE:

$$E_{\rm OPE} = C[P_A(11) - 3P_A(10) - 3P_A(01) + 9P_A(00)], \quad (8)$$

where C is a constant in units of energy. A value $C \sim 1.5$ MeV gives a reasonably good average scale factor. This expression reflects the fact that S-wave NN interactions are attractive while P-wave interactions are repulsive. It does not attempt to differentiate between ${}^1S_0$ and ${}^3S_1 - {}^3D_1$ channels, when in reality the former is just unbound and the latter produces a bound deuteron, thanks largely to the OPE tensor force. However, it does reflect the large difference between the weakly repulsive ${}^3P_J$ channels and the strongly repulsive ${}^1P_1$ interaction. We will find that this simple expression does a remarkably good job of predicting overall trends in binding and relative stability for s- and p-shell nuclei, as well as explaining a variety of observed features in the excitation spectra.

III. ENERGY SPECTRA

The $P_A(ST)$ and $E_{\rm OPE}$ for $A = 2$–5 nuclei are shown in Table I. (In the following tables, only the most neutron-rich member of any isobaric multiplet is shown, e.g., ^{3}H but not ^{3}He, and ^{6}He but not ^{6}Be or the isobaric analog states in ^{6}Li; they should be understood to be essentially the same for nuclear forces and differ primarily by the Coulomb energy.) The deuteron ^{2}H has only one $ST = 10$ pair, to which is assigned the strength $-3C$. In our simple model, the $ST = 01$ dineutron would also be bound, whereas in reality it is just unbound, and is not shown. The triton ^{3}H has three pairs, equally divided between $ST = 10$ and 01 according to Eqs. (4)–(7), and thus gets a strength of $-9C$, while the α, ^{4}He has six such pairs with a total strength of $-18C$.

If we use $E_{\rm OPE}$ to judge the relative binding of these nuclei, then the d:t:α energies should be in the ratio 1:3:6, whereas in reality they are more like 1:4:13. Of course, the binding is the result of a cancellation between kinetic and potential energies, and $E_{\rm OPE}$ is essentially a potential measure. In fact, GFMC calculations for the AV18/IL2 Hamiltonian give the expectation values for the two-body potential to be in the ratio 1:2.7:6.3 for these nuclei [5], reasonably close to $E_{\rm OPE}$. The $E_{\rm OPE}$ will be a useful gauge for binding energies only if there is something like a virial theorem for nuclei that says the kinetic and potential energies are proportional to each other. Fortunately there does seem to be such a relation, at least in the light p-shell nuclei, as shown by the results of GFMC calculations displayed in Table II. For $6 \leqslant A \leqslant 12$ nuclei, the ratio $R_{\rm KV}$, of kinetic- to potential-energy expectation values

TABLE I. Pairs and OPE weights for $A = 2$–5 nuclei.

ST	^{2}H	^{3}H	^{4}He	^{5}He	
	${}^3S[2]$	${}^2S[3]$	${}^1S[4]$	${}^2P[41]$	
	ss	ss	ss	ss	sp
11					$^9/_4$
10	1	$^3/_2$	3	3	$^3/_4$
01		$^3/_2$	3	3	$^3/_4$
00					$^1/_4$
P_A	1	3	6	6	4
$E_{\rm OPE}$	$-3C$	$-9C$	$-18C$	$-18C$	0

TABLE II. Ratio of kinetic to potential energy for $A \leqslant 12$ nuclei from GFMC calculations with the AV18/IL2 Hamiltonian.

^{A}Z	$R_{\rm KV}$	^{A}Z	$R_{\rm KV}$
^{2}H	0.90	^{8}Li	0.79
^{3}H	0.84	^{8}Be	0.76
^{4}He	0.75	^{9}He	0.81
^{6}He	0.78	^{9}Li	0.79
^{6}Li	0.79	^{9}Be	0.77
^{7}He	0.79	^{10}Be	0.77
^{7}Li	0.78	^{10}B	0.77
^{8}He	0.80	^{12}C	0.77

varies only from 0.76 to 0.81, while there is a much greater range of 0.75 to 0.90 for the *s*-shell nuclei. We note that the lowest ratios occur for the most spatially symmetric nuclei ^{4}He, ^{8}Be, and ^{12}C, as we might expect.

A further complication is that, when realistic tensor forces are included, some fraction of the $ST = 01$ pairs will be converted to 11 pairs, and a small fraction of $ST = 10$ pairs to 00 pairs, because of multibody correlations. Variational Monte Carlo (VMC) calculations for ^{4}He found the actual distribution of 11:10:01:00 pairs to be 0.47:2.53:2.99:0.01 [23]. For our simple model we focus on the distribution of pairs before such mixing takes place.

While this very qualitative model is not particularly useful for the *s* shell, it starts to have some utility in the *p* shell. The 10 pairs of nucleons in ^{5}He are divided into six pairs within the *s* shell, designated *ss* in Table I, and four pairs with one nucleon in the *s* shell and one in the *p* shell, designated *sp*. The *ss* pairs are distributed exactly as in ^{4}He, while the *sp* pairs come in just the right combination to give no additional contribution to $E_{\rm OPE}$. Thus the prediction is that ^{5}He should have the same binding as ^{4}He, when in fact it is unstable against breakup by $\sim$1 MeV. For cases like this, our simple measure is not sufficient to determine stability, but only to indicate a situation that could go either way, depending on, for example, how much the virial ratio $R_{\rm KV}$ of Table II varies. In the case of ^{5}He, the residual attraction from shorter-range *NN* and $3N$ forces is not enough to overcome the additional kinetic energy that is generated by the requirement of putting the fifth nucleon in a *p*-shell orbital.

For $A = 6$ nuclei, shown in Table III, the s-shell core remains the same, while the number of *sp* pairs doubles, but still with no net contribution to $E_{\rm OPE}$. Effectively, the *s* and *p* shells decouple from each other at the OPE level. The final energy of ^{6}Li and ^{6}He then depends on the last pair of nucleons that is wholly within the *p* shell, designated *pp* in Table III. Starting with $A = 6$, there are multiple ways of adding up orbital and spin angular momenta to get the total $J^{\pi}; T$ of a given nuclear state [24]; they are labeled by their *LS* coupling and spatial symmetry, $^{2S+1}L[n]$, and all allowed *L* values are listed. For ^{6}Li this last pair can be part of a $^{3}S[42]$ or $^{3}D[42]$ state (essentially a deuteron with orbital momentum of 0 or 2 around an α core) with an associated strength of $-3C$, or the last pair can be part of a $^{1}P[411]$ state, which contributes $+9C$ to our binding measure. The total $E_{\rm OPE}$ for ^{6}Li is the sum of the *ss* and *pp* pairs, or $-21C$ for the [42] states and $-9C$ for the [411] state. For ^{6}He the last pair can be part of either a $^{1}S[42]$ or $^{1}D[42]$ state (essentially a spin-zero dineutron with $L = 0$ or 2 around an α core) with strength $-3C$, or part of a $^{3}P[411]$ state with strength $+C$; the corresponding total $E_{\rm OPE}$ is $-21C$ or $-17C$, respectively.

TABLE III. Pairs and OPE weights for $A = 6$ nuclei. The $E_{\rm OPE}$ weight does not depend on the total *L* value, but all possible values for a given spin and spatial symmetry combination are enumerated the allowed $T = 0$ states are given under the ^{6}Li header and the $T = 1$ states under the ^{6}He header.

ST			^{6}Li		^{6}He	
			$^{3}SD[42]$	$^{1}P[411]$	$^{1}SD[42]$	$^{3}P[411]$
	ss	*sp*	*pp*	*pp*	*pp*	*pp*
11		$^{9}/_{2}$				1
10	3	$^{3}/_{2}$	1			
01	3	$^{3}/_{2}$			1	
00		$^{1}/_{2}$		1		
P_A	6	8	1	1	1	1
$E_{\rm OPE}$	$-18C$	0	$-3C$	$+9C$	$-3C$	$+1C$

Thus the prediction of our simple model is that ^{6}Li and ^{6}He ground states should have [42] symmetry, with about the same energy, and be weakly bound compared with ^{4}He, which is pretty much correct, given the above a caveat about a unbound dineutron and bound deuteron. The experimental spectrum [25] is shown in Fig. 1, where the levels are labeled by their dominant symmetry. The ^{6}Li ground state is 1.47 MeV below the α-deuteron threshold, while ^{6}He is 0.97 MeV below the α-dineutron threshold. GFMC calculations indicate that much of the binding between clusters is provided by the $3N$ force; if only the AV18 *NN* force is used, ^{6}Li is stable by 0.6 MeV and ^{6}He is unstable by 0.3 MeV [10].

Not surprisingly, in the excitation spectrum the *D* states are higher than the *S* states, because the angular-momentum

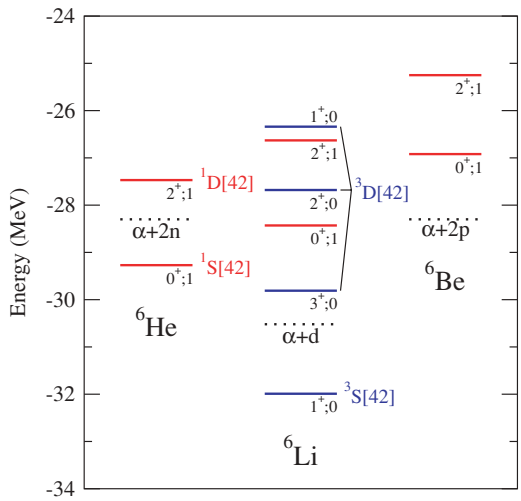

FIG. 1. (Color online) Experimental spectrum for $A = 6$ nuclei; $T = 0$ ($T = 1$) states are shown by blue (red) solid lines and breakup thresholds by black dotted lines.

TABLE IV. Pairs and OPE weights for $A = 7$ nuclei.

ST			^{7}Li				^{7}He	
			$^2PF[43]$	$^4PD[421]$	$^2PD[421]$	$^2S[4111]$	$^2PD[421]$	$^4S[4111]$
	ss	sp	pp	pp	pp	pp	pp	pp
11		$^{27}/_4$		$^3/_2$	$^3/_4$	$^3/_2$	$^3/_2$	3
10	3	$^9/_4$	$^3/_2$	$^3/_2$	$^3/_4$			
01	3	$^9/_4$	$^3/_2$		$^3/_4$		$^3/_2$	
00		$^3/_4$			$^3/_4$	$^3/_2$		
P_A	6	12	3	3	3	3	3	3
$E_{\rm OPE}$	$-18C$	0	$-9C$	$-3C$	$+3C$	$+15C$	$-3C$	$+3C$

barrier screens some of the overall potential attraction. In shell-model studies this feature is taken into account by the inclusion of an L^2 term in the interaction [26], but the spread between different L states of the same spatial symmetry is generally smaller than the spacing between different spatial symmetry groups, and here we are after only the most general nuclear structure aspects. Further, the ^3D combination in ^{6}Li is split into $J = 1,2,3$ states ordered with maximum J lowest, as dictated by the spin-orbit force. The antisymmetric [411] states are several MeV higher in the spectrum, and no corresponding experimental states have been identified. However, our simple model predicts that the antisymmetric $^1P[411]$ state in ^{6}Li is much higher than the $^3P[411]$ state in ^{6}He, which suggests that when configuration mixing with tensor forces is done, the admixture of these components in the respective ground states will be less for ^{6}Li than for ^{6}He. This is borne out in VMC diagonalizations with realistic forces in which the amplitudes of the different components in the ground state are 0.98:0.14:0.10 for the $^3S[42]$:$^3D[42]$:$^1P[411]$ pieces in ^{6}Li and 0.97:0.23 for the $^1S[42]$:$^3P[411]$ pieces in ^{6}He [10].

The $P_A(ST)$ and $E_{\rm OPE}$ for $A = 7$ nuclei are given in Table IV. Again we see that the s-shell core gives the same contribution as before, and though there are now 12 sp pairs, they continue to give no net contribution to $E_{\rm OPE}$. All the action is now in the three pp pairs. In ^{7}Li they can form part of a maximally symmetric $^2P[43]$ or $^2F[43]$ state with energy contribution $-9C$ for a total $E_{\rm OPE} = -27C$, which equals the sum of α and triton energies; experimentally the ground state is 2.47 MeV below this sum, as seen in the experimental spectrum of Fig. 2. Again, much of the binding between clusters is apparently due to the $3N$ forces; GFMC calculations with AV18 alone produce a ^{7}Li ground state only 0.3 MeV below the α-triton threshold [10].

As labeled in the figure, the ^{7}Li states are ordered according to our simple model, with $^2P[43]$ and $^2F[43]$ states lowest, followed by the $^4P[421]$ states and the start of the $^4D[421]$ states; VMC calculations confirm that these are by far the dominant components of the first eight states. (The lowest five states in ^{7}Be follow a similar pattern with a Coulomb shift; the higher states may not be as well known experimentally.) The $^4P[421]$ states have a net $E_{\rm OPE} = -21C$, the same as that of ^{6}Li ground state, and they lie just above the threshold for breakup into $^6\text{Li} + n$. The $^2P[421]$ and $^4P[421]$ $T = 1/2$ states in ^{7}Li have the same spatial symmetry but the former contain an admixture of the very repulsive $ST = 00$ pairs, which pushes their energy up significantly, and no corresponding experimental states have been identified. In contrast, the $^2P[421]$ $T = 3/2$ ground state in ^{7}He (and its isobaric analogs) does not have any $ST = 00$ pp pairs and by our simple model has the same energy as the ^{6}He ground state, which is about right.

The $P_A(ST)$ and $E_{\rm OPE}$ for $A = 8$ nuclei are given in Tables V and VI. In the former the ss and sp pairs are shown again to remind us that each of the p-shell nuclei has an s-shell core contributing $-18C$ to $E_{\rm OPE}$ and no contribution from the sp pairs. In ^{8}Be the six pp pairs in the maximally symmetric

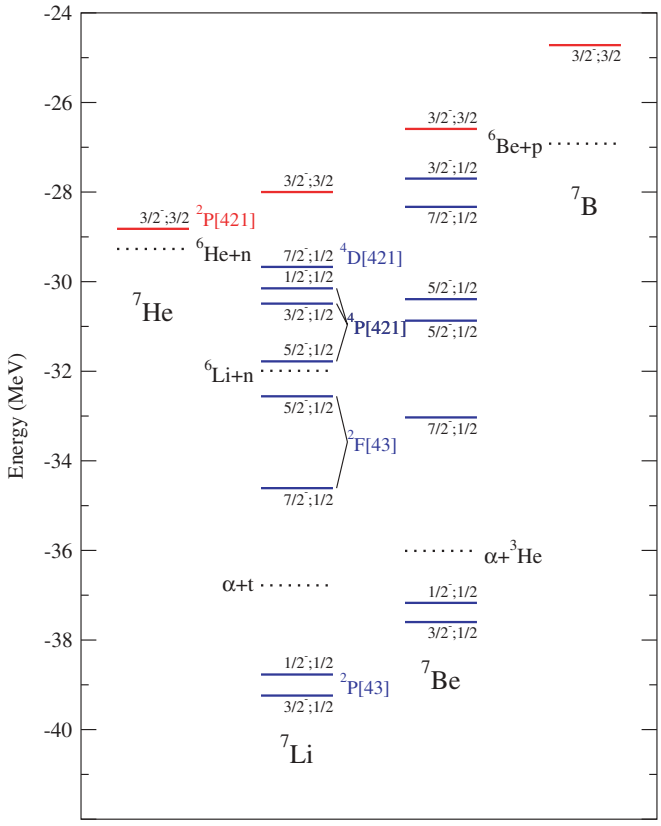

FIG. 2. (Color online) Experimental spectrum for $A = 7$ nuclei; $T = 1/2$ ($T = 3/2$) states are shown by blue (red) solid lines.

TABLE V. Pairs and OPE weights for ^{8}Be.

ST			^{8}Be				
			^1SDG[44]	^3PDF[431]	^5SD[422]	^1SD[422]	^3P[4211]
	ss	sp	pp	pp	pp	pp	pp
11		9		$^3/_2$	3	$^3/_2$	$^5/_2$
10	3	3	3	$^5/_2$	3	$^3/_2$	$^3/_2$
01	3	3	3	$^3/_2$		$^3/_2$	$^1/_2$
00		1		$^1/_2$		$^3/_2$	$^3/_2$
P_A	6	16	6	6	6	6	6
$E_{\rm OPE}$	$-18C$	0	$-18C$	$-6C$	$-6C$	$+6C$	$+10C$

[44] ground state effectively form a second α, so the total $E_{\rm OPE}$ is $2(-18C) = -36C$, compared with $-28C$ for ^{8}Li and $-24C$ for ^{8}He ground states. This is a fair representation of the spread in the experimental spectrum, shown in Fig. 3 [27]. The ^{8}Be ground state is practically degenerate with the energy of two α's, ^{8}Li is significantly less bound, but is a little more bound than ^{7}Li ($-27C$), and ^{8}He is somewhat less bound, but below ^{6}He and ^{7}He (both $-21C$). The increased binding for ^{8}He is essentially due to the completion of a second dineutron pair in its [422] symmetry ground state, which is worth an additional $-3C$ in $E_{\rm OPE}$.

The gap between the [44] and [431] symmetry states in ^{8}Be has the large value of $12C$, suggesting little mixing between them, and VMC calculations indicate the first 0^+, 2^+, and 4^+ states are ∼99% pure symmetry [44]. By comparison, the small energy gap of $4C$ between the [422] and [4211] symmetry states in ^{8}He leads to mixed amplitudes of 0.8:0.6 in its ground state [10]. In ^{8}Li there are both triplet and singlet states of symmetry [431], but the higher spin states fall lower in the spectrum because they avoid the repulsive $ST = 00$ pairs; the same is true for the three different spin states of [4211] symmetry and in ^{8}Be for the two different spin states of [422] symmetry.

The $P_A(ST)$ and $E_{\rm OPE}$ in $A = 9$ nuclei are given in Tables VII and VIII. With the contribution from the s-shell core added in, the $E_{\rm OPE}$ are $-36C$, $-30C$, and $-24C$ for the ground states of ^{9}Be, ^{9}Li, and ^{9}He, respectively, which is again a very good approximation to the experimental spectrum shown in Fig. 4 [27]. The ^{9}Be ground state is predicted to have the same energy as ^{8}Be or two α's: The addition of one nucleon to the ground state of ^{8}Be generates four new pp pairs in ^{9}Be, but with just the right combination to add no additional binding to $E_{\rm OPE}$. Experimentally ^{9}Be is bound with respect to the threshold for α-α–neutron breakup by 1.57 MeV, which in turn is 0.10 MeV below the ^{8}Be + n threshold. GFMC calculations indicate that the stability of the last neutron is again due to $3N$ forces: Whereas the AV18/IL2 Hamiltonian gets 1.9 ± 0.5 MeV for the binding relative to ^{8}Be, AV18 alone is stable by only 0.1 ± 0.4 MeV [9,10].

The ^{9}Li ground state is predicted to be somewhat more bound with respect to ^{8}Li ($-30C$ compared with $-28C$), and experimentally it is stable by 4.06 MeV. On the other hand, ^{9}He is predicted to be the same energy as ^{8}He (both $-24C$) because the last neutron is unpaired; experimentally the lowest natural-parity $1/2^-$ state is unbound by ∼1.2 MeV. However, recent experiments indicate the lowest state in ^{9}He is an unnatural positive-parity $1/2^+$ state just above threshold, and there are also many low-lying positive-parity states in ^{9}Be, starting with a $1/2^+$ state just above the $2\alpha + n$ threshold. One can construct these unnatural-parity states by putting the last nucleon in an sd-shell orbital outside the p-shell core. As with the p shell, the $E_{\rm OPE}$ weight factor is such that there is no net interaction between an sd-shell nucleon and the core. In the cases of ^{9}He and ^{9}Be, our simple model suggests that the the long-range part of the NN potential does not care what orbital the last nucleon goes into; whether a p-shell or sd-shell orbital is more stable depends on the residual shorter-range NN interaction, the $3N$ interaction, and the kinetic-energy cost.

TABLE VI. Pairs and OPE weights for ^{8}Li and ^{8}He.

ST	^{8}Li						^{8}He	
	^3PDF[431]	^1PDF[431]	^3SD[422]	^5P[4211]	^3P[4211]	^1P[4211]	^1SD[422]	^3P[4211]
	pp	pp	pp	pp	pp	pp	pp	pp
11	2	$^3/_2$	$^5/_2$	4	3	$^5/_2$	3	4
10	2	$^3/_2$	$^3/_2$	2	1	$^1/_2$		
01	2	$^5/_2$	$^3/_2$		1	$^3/_2$	3	2
00		$^1/_2$	$^1/_2$		1	$^3/_2$		
P_A	6	6	6	6	6	6	6	6
$E_{\rm OPE}$	$-10C$	$-6C$	$-2C$	$-2C$	$+6C$	$+10C$	$-6C$	$-2C$

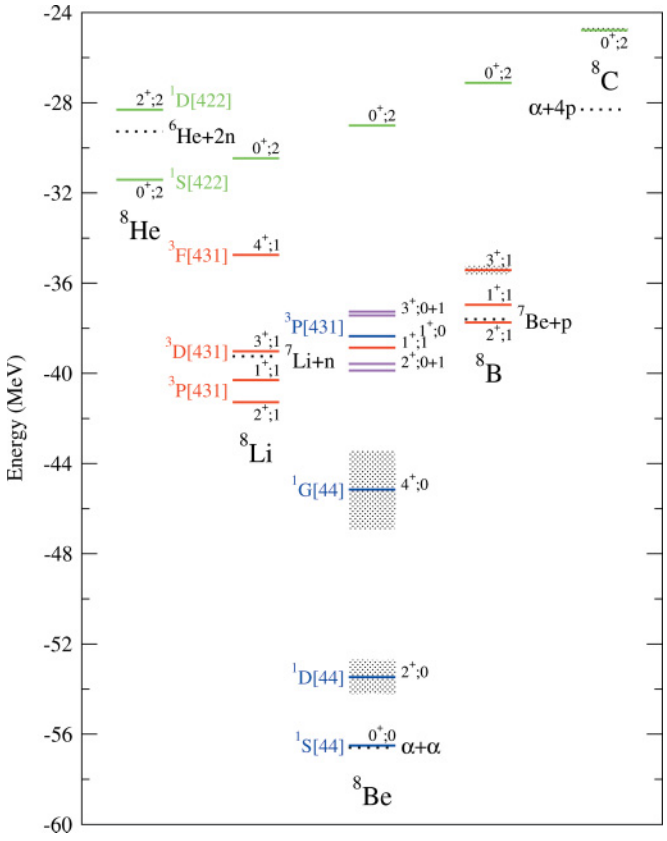

FIG. 3. (Color online) Experimental spectrum for $A = 8$ nuclei: $T = 0$, 1, and 2 states are shown by blue, red, and green solid lines, respectively, and isospin mixed states by magenta lines.

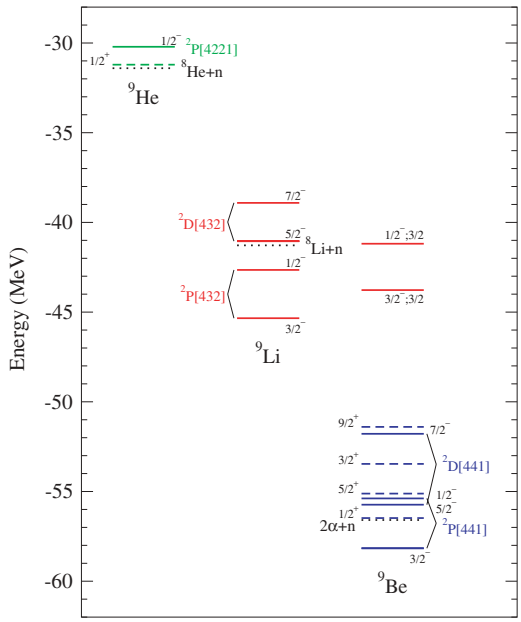

FIG. 4. (Color online) Experimental spectrum for $A = 9$ nuclei: $T = 1/2$, 3/2, and 5/2 states are shown by blue, red, and green lines respectively; solid lines denote natural-parity states and dashed lines unnatural-parity states.

There is a moderate gap of size $6C$ between the first and second symmetry states in ^{9}Be, which is not as large as the gap in ^{8}Be; consequently the low-lying states are mostly [441] symmetry with relatively small admixtures of [432] components, but not as pure as the ^{8}Be [44] states [9]. The smaller gap between symmetry states in ^{9}Li leads to more mixing of the [432] and [4311] components there. VMC diagonalizations also continue to show that, for states of the same spatial symmetry, those with higher spin lie lower in the spectrum, again because of a smaller presence of repulsive $ST = 00$ pairs.

The $P_A(ST)$ and $E_{\rm OPE}$ in $A = 10$ nuclei are shown in Tables IX–XI. The $E_{\rm OPE}$ are $-27C$, $-31C$, $-39C$, and $-39C$ for ^{10}He, ^{10}Li, ^{10}Be, and ^{10}B, respectively. Thus ^{10}B and ^{10}Be should have the same binding, which experimentally they do at 64.75 and 64.98 MeV, as seen in Figs. 5 and 6. They are predicted to be about 4–5 MeV more bound than ^{8}Be and ^{9}Be, but experimentally it is more like 7–8 MeV. On the other hand, the prediction for ^{10}Li is that it should be a little more bound than ^{9}Li, whereas it is unbound by about 0.25 MeV. Further, ^{10}He should be bound by several mega-electron-volts compared with ^{8}He and ^{9}He by the completion of another dineutron pair, whereas it is unbound by 1 MeV compared with ^{8}He. This could be an indication that jj coupling is starting to be more appropriate as the neutron p shell is completed [28], with this last pair of neutrons being a $p_{1/2}$ pair that joins at a noticeably higher energy than the first two dineutrons. ^{10}Li and ^{10}He are the only two nuclei out of 27 in the p shell

TABLE VII. Pairs and OPE weights for ^{9}He and ^{9}Li.

ST			^{9}He	^{9}Li				
			^2P[4221]	^2PDF[432]	^4SD[4311]	^2SD[4311]	^4P[4221]	^2P[4221]
	ss	sp	pp	pp	pp	pp	pp	pp
11		$^{45}/_4$	6	$^{15}/_4$	5	$^{17}/_4$	$^{11}/_2$	$^{19}/_4$
10	3	$^{15}/_4$		$^9/_4$	$^5/_2$	$^7/_4$	2	$^5/_4$
01	3	$^{15}/_4$	4	$^{15}/_4$	$^5/_2$	$^{13}/_4$	2	$^{11}/_4$
00		$^5/_4$		$^1/_4$		$^3/_4$	$^1/_2$	$^5/_4$
P_A	6	20	10	10	10	10	10	10
$E_{\rm OPE}$	$-18C$	0	$-6C$	$-12C$	$-10C$	$-4C$	$-1C$	$+4C$

TABLE VIII. Pairs and OPE weights for ^{9}Be.

ST	^{9}Be							
	$^2PDFG[441]$	$^4PDF[432]$	$^2PDF[432]$	$^4SD[4311]$	$^2SD[4311]$	$^6P[4221]$	$^4P[4221]$	$^2P[4221]$
	pp	pp	pp	pp	pp	pp	pp	pp
11	$^9/_4$	$^{15}/_4$	3	$^{17}/_4$	$^7/_2$	6	$^{19}/_4$	4
10	$^{15}/_4$	$^{15}/_4$	3	$^{13}/_4$	$^5/_2$	4	$^{11}/_4$	2
01	$^{15}/_4$	$^9/_4$	3	$^7/_4$	$^5/_2$		$^5/_4$	2
00	$^1/_4$	$^1/_4$	1	$^3/_4$	$^3/_2$		$^5/_4$	2
P_A	10	10	10	10	10	10	10	10
$E_{\rm OPE}$	$-18C$	$-12C$	$-6C$	$-4C$	$+2C$	$-6C$	$+4C$	$+10C$

(not counting isobaric analogs) that are falsely predicted to be stable by our simple model.

Comparing the different symmetry states in Table XI for ^{10}B, we see that the [442] components are $12C$ below the [4411], [433], etc., components, so there is very little admixture of the latter into the lowest-lying states. However, in ^{10}Be the gap between the ground-state [442] symmetry and the [4411] and [433] components is only $4C$, so there is a moderate admixture into the ground state [9]. The clearest signature for a state of these next spatial symmetries in the p shell would be a 1^+ state in ^{10}Be, expected at $\sim$6 MeV excitation, but no such state has been observed. However, unnatural-parity states that involve an sd-shell intruder are now low enough in the spectrum for some of them to be particle stable; discussion of these is deferred to the next section.

In full GFMC calculations, the $3N$ force starts to make an especially large impact by $A = 10$ in that it starts to reorder some of the states from our simple expectations. Naively we would expect the ^{10}B spectrum to be something like ^{6}Li, with a 1^+ $^3S[442]$ ground state, and a collection of $3^+, 2^+$, and 1^+ states above coming from the spin-orbit splitting of the $^3D[442]$ state. The situation is complicated by the fact that there are two linearly independent ways to construct an $L = 2$ [442] symmetry state in the p shell. With AV18 only, the ground state of ^{10}B is in fact a 1^+ state, but for AV18/IL2, the spin-orbit splitting of the ^{3}D[442] states is large enough that one of the 3^+ states is lowered to become the ground state [9], as observed experimentally. Similar results are obtained in NCSM calculations by use of the CD-Bonn or AV8′

TABLE IX. Pairs and OPE weights for ^{10}He and ^{10}Li states.

ST			^{10}He	^{10}Li		
			$^1S[4222]$	$^3PD[4321]$	$^1PD[4321]$	$^3S[4222]$
	ss	sp	pp	pp	pp	pp
11		$^{27}/_2$	$^{29}/_4$	$^{27}/_4$	8	9
10	3	$^9/_2$	$^{11}/_4$	$^9/_4$	2	
01	3	$^9/_2$	$^{19}/_4$	$^{21}/_4$	4	6
00		$^3/_2$	$^1/_4$	$^3/_4$	1	
P_A	6	24	15	15	15	15
$E_{\rm OPE}$	$-18C$	0	$-9C$	$-13C$	$-9C$	$-1C$

NN potentials versus AV8′ with the TM′(99) $3N$ potential added [13,14]. By comparison, ^{10}Be behaves more like what we expect, with a 0^+ ground state that is predominantly $^1S[442]$ symmetry in character, while the next two 2^+ excited states are dominated by the two $^1D[442]$ symmetry combinations.

The complicated spectrum for ^{10}B is shown in detail in Fig. 6. Based on GFMC calculations, the two $^3D[442]$ triplets can be sorted by their quadrupole moments Q. One triplet with large positive Q is widely split and contains the ground state, the second 2^+ near 6 MeV excitation, and a predicted, but unobserved, fourth 1^+ near 8 MeV. The other triplet has smaller negative Q and is closely spaced, starting with the second 1^+ at 2-MeV excitation, followed by the first 2^+ and second 3^+. The first 1^+ is the $^3S[442]$ state, while the third 1^+ around 5 MeV excitation (marked by a dash-dotted line in the figure) is believed to be a $2\hbar\omega$ excitation. Likewise, the second 0^+ in ^{10}Be near 6-MeV excitation is believed to be a

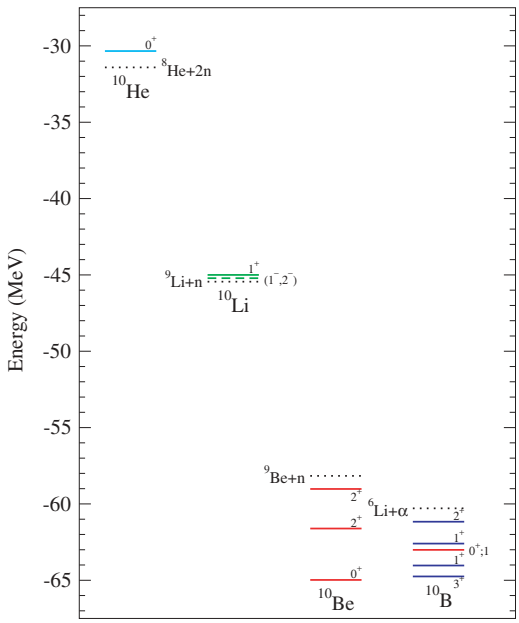

FIG. 5. (Color online) Simplified experimental spectrum for $A = 10$ nuclei; only stable natural-parity states are shown for ^{10}Be and ^{10}B.

TABLE X. Pairs and OPE weights for ^{10}Be states.

ST	^{10}Be							
	$^1SD^*FG[442]$	$^3PF[4411]$	$^3PF[433]$	$^5PD[4321]$	$^3P^*D^*[4321]$	$^1PD[4321]$	$^5S[4222]$	$^1S[4222]$
	pp	pp	pp	pp	pp	pp	pp	pp
11	$^9/_2$	$^{11}/_2$	$^{11}/_2$	$^{29}/_4$	$^{25}/_4$	$^{23}/_4$	8	$^{13}/_2$
10	$^9/_2$	$^9/_2$	$^9/_2$	$^{19}/_4$	$^{15}/_4$	$^{13}/_4$	4	$^5/_2$
01	$^{11}/_2$	$^9/_2$	$^9/_2$	$^{11}/_4$	$^{15}/_4$	$^{17}/_4$	2	$^7/_2$
00	$^1/_2$	$^1/_2$	$^1/_2$	$^1/_4$	$^5/_4$	$^7/_4$	1	$^5/_2$
P_A	15	15	15	15	15	15	15	15
$E_{\rm OPE}$	$-21C$	$-17C$	$-17C$	$-13C$	$-5C$	$-1C$	$-1C$	$+11C$

*Denotes two linearly independent combinations.

$2\hbar\omega$ state. These latter states will be discussed below with the unnatural-parity states.

The $A = 10$ nuclei are the halfway points in the p shell; moving further up in the shell is comparable with removing particles from the filled [4444] state of ^{16}O. The $A = 11$ nuclei are the five-hole complements of the five- (p-shell) particle $A = 9$ nuclei, $A = 12$ nuclei are complements of $A = 8$, etc. For example, ^{11}B is the complement of ^{9}Be with the same allowed set of ^{2S+1}L components, except that [441] symmetry becomes [443], [432] becomes [4421], [4311] becomes [4331], and [4221] becomes [4322]. In like manner, ^{11}Be is the complement of ^{9}Li, and ^{11}Li is the complement of ^{9}He. Consequently tables are not given for these heavier nuclei, except for ^{12}C, which is of particular interest as it is at the present limits of GFMC and NCSM calculations with realistic forces [11,12], as well as being an extremely popular experimental target.

Table XII shows that ^{12}C has exactly the same ^{2S+1}L combinations as ^{8}Be, with spatial symmetries augmented by an additional [4] in the Young diagram. The ground state will be a $^1S[444]$ 0^+ state with $E_{\rm OPE} = 3(-18) = -54C$ three times that of ^{4}He. Experimentally ^{12}C is 7 MeV or 8% more bound than three α's. The distribution of the 28 pp pairs is such that 16 average to give zero contribution to $E_{\rm OPE}$ leaving 12 $ST = 10$ and 01 pairs that are equivalent to two α's in the p shell. In this simple model every time an α is formed in the p shell, it effectively decouples from other nucleons

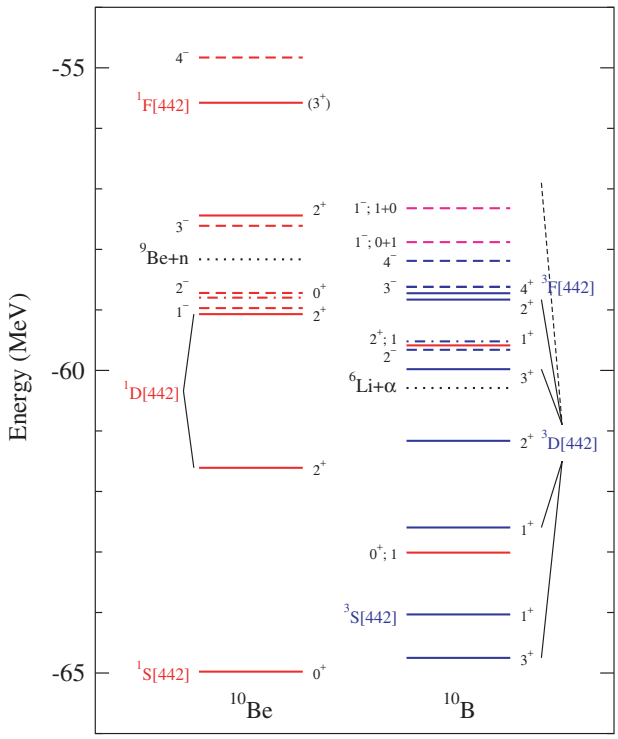

FIG. 6. (Color online) Detailed experimental spectrum for ^{10}Be and ^{10}B nuclei.

TABLE XI. Pairs and OPE weights for ^{10}B states.

ST	^{10}B						
	$^3SD^*FG[442]$	$^1PF[4411]$	$^1PF[433]$	$^5PD[4321]$	$^3PD[4321]$	$^7S[4222]$	$^3S[4222]$
	pp	pp	pp	pp	pp	pp	pp
11	$^9/_2$	$^9/_2$	$^9/_2$	$^{27}/_4$	$^{23}/_4$	9	$^{13}/_2$
10	$^{11}/_2$	$^9/_2$	$^9/_2$	$^{21}/_4$	$^{17}/_4$	6	$^7/_2$
01	$^9/_2$	$^9/_2$	$^9/_2$	$^9/_4$	$^{13}/_4$		$^5/_2$
00	$^1/_2$	$^3/_2$	$^3/_2$	$^3/_4$	$^7/_4$		$^5/_2$
P_A	15	15	15	15	15	15	15
$E_{\rm OPE}$	$-21C$	$-9C$	$-9C$	$-9C$	$-1C$	$-9C$	$+11C$

*Denotes two linearly independent combinations.

TABLE XII. Pairs and OPE weights for ^{12}C states.

ST			^{12}C				
			$^1SDG[444]$	$^3PDF[4431]$	$^5SD[4422]$	$^1SD[4422]$	$^3P[4332]$
	ss	sp	pp	pp	pp	pp	pp
11		18	9	$^{21}/_2$	12	$^{21}/_2$	$^{23}/_2$
10	3	6	9	$^{17}/_2$	9	$^{15}/_2$	$^{15}/_2$
01	3	6	9	$^{15}/_2$	6	$^{15}/_2$	$^{13}/_2$
00		2	1	$^3/_2$	1	$^5/_2$	$^5/_2$
P_A	6	32	28	28	28	28	28
$E_{\rm OPE}$	$-18C$	0	$-36C$	$-24C$	$-24C$	$-12C$	$-8C$

in the p shell. There is again a large energy gap between the first and second symmetry components in ^{12}C, so we expect the ground and low-lying states to have predominantly [444] symmetry. By contrast, we can predict that ^{12}B and ^{12}Be should have substantial mixing of different symmetries in their ground states. This knowledge is of practical benefit for the quantum Monte Carlo calculations, for which allowing for all the possible spatial symmetries in $A = 12$ nuclei is computationally prohibitive at present.

The total energy for 30 s- and p-shell nuclei, ordered by increasing A, Z but not including isobaric analogs, is plotted in Fig. 7, where experiment and our $E_{\rm OPE}$ are compared. For this figure, the coefficient in Eq.(8) has been set to be $C = 1.5$ MeV. The figure shows that up to $A \approx 9$ the simple model works quite well, but then starts to underestimate the overall binding as A increases. Considering the necessity of including $3N$ forces in full GFMC and NCSM calculations to obtain the empirical binding energies, it is not surprising that a simple model based on pairwise forces will start to fail in this manner. Cohen and Kurath in their study of effective interactions for the p shell [29] found it difficult to fit all $6 \leqslant A \leqslant 16$ nuclei at the same time, and consequently made some models to fit only $A \geqslant 8$ states. They also found in their studies of spectroscopic factors [28] that there is a gradual transition from LS coupling to jj coupling over the range $A = 9$–14, and perhaps this transition is not unrelated to the increasing importance of $3N$ forces.

As mentioned above, our simple model also predicts ^{10}He and ^{10}Li to be definitely stable when they are not. In a number of other cases, the model gives identical energies for neighboring nuclei, such as ^{4,5}He and ^{8,9}Be, and cannot predict stability one way or the other; this will be determined by finer details of the NN and $3N$ forces and kinetic-energy considerations. Nevertheless, the simple formula reproduces the experimental trends fairly well.

The model naturally indicates that total energies are close to those of summed α, t, and d subclusters, where applicable. In fact, the following energy relations hold for the maximally symmetric states with $N \geqslant Z$:

$$E(AZ = m\alpha) = E(AZ = m\alpha + n) = mE_\alpha, \quad (9)$$

$$E(AZ = m\alpha + 2n) = E(AZ = m\alpha + 3n) = mE_\alpha + E_{2n}, \quad (10)$$

$$E(AZ = m\alpha + 4n) = E(AZ = m\alpha + 5n) = mE_\alpha + 2E_{2n}, \quad (11)$$

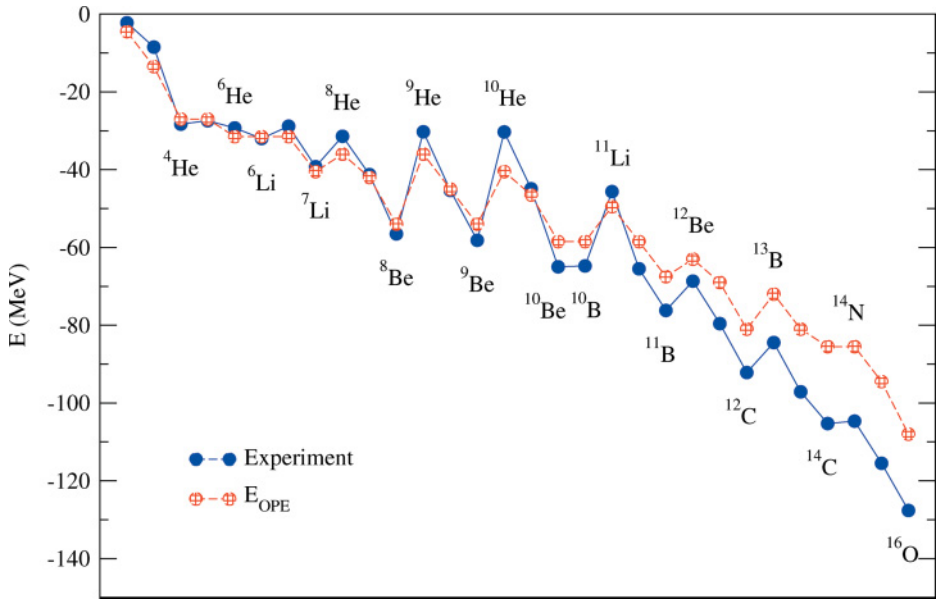

FIG. 7. (Color online) Ground-state binding energies for $A \leqslant 16$ s- and p-shell nuclei.

$$E(AZ = m\alpha + 6n) = mE_\alpha + 3E_{2n}, \quad (12)$$

$$E(AZ = m\alpha + d) = mE_\alpha + E_d, \quad (13)$$

$$E(AZ = m\alpha + t) = mE_\alpha + E_t, \quad (14)$$

$$E(AZ = m\alpha + t + n) = mE_\alpha + E_t - C, \quad (15)$$

$$E(AZ = m\alpha + t + 2n) = mE_\alpha + E_t + E_{2n}, \quad (16)$$

$$E(AZ = m\alpha + t + 3n) = mE_\alpha + E_t + E_{2n} - C, \quad (17)$$

$$E(AZ = m\alpha + t + 4n) = mE_\alpha + E_t + 2E_{2n}, \quad (18)$$

where m is the number of included α's, and $E_{2n} = -3C$ is the energy of a dineutron, which again in this simple model is equal to E_d. Two nontrivial cases are Eqs. (15) and (17), which in the p shell would apply to ^{8,10}Li and ^{12}B. The model indicates there is a little extra binding, C more than the sum of the subclusters, on the addition of the last neutron. This is an accurate description of experiment for ^{8}Li and ^{12}B, but not for ^{10}Li.

IV. BEYOND THE *p* SHELL

This simple model can be extended into the *sp* shell, although the utility of doing so will continue to diminish as A increases. Counting pairs among the s, p, and sd shells, the contributions to $E_{\rm OPE}$ again average out so there is no net interaction between the shells. Then the progression from ^{16}O to ^{17}O, ^{18}O, and ^{18}F nuclei is exactly analogous to the progression from ^{4}He to ^{5}He, ^{6}He, and ^{6}Li. This is in rough accord with experiment, as is the prediction that the multiple-α nuclei will continue as Eq. (9). However, it will also predict that ^{19}F is definitely more bound than ^{20}O, which is not the case; among other things, Coulomb effects are becoming important enough that they need to be treated explicitly.

However, the basic logic of this simple model may be applicable to *sd*-shell, intruder states in the p shell. The intruder states in $A = 10$ nuclei, in which particle-stable intruders first occur, are an example. An interesting feature of the data is that the intruders in ^{10}Be are ordered starting from the most bound level as 1^-, 2^-, 3^-, and 4^-. However, in ^{10}B the order is 2^-, 3^-, 4^-, and then 1^-. The relative ordering of the 1^- and 2^- states in these nuclei can be understood in the following manner. A major part of the $A = 9$ ground state is ^{8}Be(0^+) plus an unpaired $1p$-shell nucleon ($1p_{3/2}$ orbital in jj coupling) to which we add a spin-up or spin-down $2s$-shell nucleon. Because these nucleons have on average no net interaction with the ^{8}Be core, their pairwise interaction should dominate. The 2^- state is a "stretch" state obtainable only if both spins of the pair are aligned, i.e., pure $S = 1$, while the 1^- state will have some $S = 0$ pair content. In ^{10}Be the last pair has $T = 1$, so the 2^- state will be a ^3P pair, whereas the 1^- state will be partially a ^1S pair, which is more attractive—hence the 1^- state should be lower in the spectrum. In ^{10}B the last pair has $T = 0$, so the 2^- state will be a ^3S pair, whereas the 1^- state will have some admixture of ^1P, which is (much) more repulsive—hence the 1^- state will be (much) higher. Preliminary VMC calculations with realistic interactions successfully reproduce these level orderings and exhibit exactly this type of S, T pair distribution.

One may also consider placing both last two nucleons outside the ^{8}Be core into the *sd* shell, either as a dineutron pair in ^{10}Be or a deuteron in ^{10}B. In our simple model, these would have the same energy as the ground states, although in practice there would be some reduction in binding that is due to the greater distance from the core of these orbitals and the consequent overall loss of potential attraction. In actual fact, the second 0^+ in ^{10}Be and third 1^+ in ^{10}B (shown in Fig. 6 by dash-dot lines) are believed to be $2\hbar\omega$ excitations of this type. These states pose an interesting challenge for both the GFMC and NCSM microscopic calculations.

The present simple model provides an interesting contrast to relativistic mean-field theories, which commonly omit the pion with the argument that its contribution will spin-isospin average to zero in nuclear matter; such models have been applied to nuclei as light as ^{16}O [30]. However, summing the expectation value of the OPE operator $\sigma_i \cdot \sigma_j \tau_i \cdot \tau_j$ over all pairs, we get a result that grows linearly with A for the multiple-α nuclei. In practice, the quantum Monte Carlo calculations with realistic forces find that OPE provides about 75% of the net potential energy expectation value, although much of this comes from the tensor part of OPE [5].

V. CONCLUSIONS

A simple model has been presented for understanding the basic structure of light nuclei. It is based on counting the number of different S, T pairs that occur in a given nuclear state of specific spatial symmetry and multiplying by a numeric strength taken from OPE. This simple picture gives a good description for the growth of binding as A increases while showing saturation as the p shell is reached. It explains the tendency of light nuclei to form d, t and α subclusters and a variety of features in the excitation spectra, including why, for states of the same spatial symmetry, those of higher S are lower in the spectrum. I hope this picture provides some useful physical intuition.

ACKNOWLEDGMENTS

I thank D. F. Geesaman, D. Kurath, D. J. Millener, V. R. Pandharipande, and S. C. Pieper for valuable discussions. This work is supported by the U.S. Department of Energy, Office of Nuclear Physics, under contract no. W-31-109-ENG-38.

[1] R. B. Wiringa, V. G. J. Stoks, and R. Schiavilla, Phys. Rev. C **51**, 38 (1995).
[2] R. Machleidt, F. Sammarruca, and Y. Song, Phys. Rev. C **53**, R1483 (1996).
[3] R. Machleidt, Phys. Rev. C **63**, 024001 (2001).
[4] V. G. J. Stoks, R. A. M. Klomp, C. P. F. Terheggen, and J. J. de Swart, Phys. Rev. C **49**, 2950 (1994).
[5] S. C. Pieper, V. R. Pandharipande, R. B. Wiringa, and J. Carlson, Phys. Rev. C **64**, 014001 (2001).
[6] S. A. Coon and H. K. Han, Few-Body Syst. **30**, 131 (2001).
[7] H. Kamad *et al.*, Phys. Rev. C **64**, 044001 (2001).
[8] S. C. Pieper and R. B. Wiringa, Annu. Rev. Nucl. Part. Sci. **51**, 53 (2001).

[9] S. C. Pieper, K. Varga, and R. B. Wiringa, Phys. Rev. C **66**, 044310 (2002).
[10] S. C. Pieper, R. B. Wiringa, and J. Carlson, Phys. Rev. C **70**, 054325 (2004).
[11] S. C. Pieper, Nucl. Phys. **A751**, 516 (2005).
[12] P. Navrátil, J. P. Vary, and B. R. Barrett, Phys. Rev. C **62**, 054311 (2000).
[13] E. Caurier, P. Navrátil, W. E. Ormand, and J. P. Vary, Phys. Rev. C **66**, 024314 (2002).
[14] P. Navrátil and W. E. Ormand, Phys. Rev. C **68**, 034305 (2003).
[15] K. Kowalski, D. J. Dean, M. Hjorth-Jensen, T. Papenbrock, and P. Piecuch, Phys. Rev. Lett. **92**, 132501 (2004).
[16] M. Wloch, D. J. Dean, J. R. Gour, M. Hjorth-Jensen, K. Kowalski, T. Papenbrock, and P. Piecuch, Phys. Rev. Lett. **94**, 212501 (2005).
[17] R. B. Wiringa and S. C. Pieper, Phys. Rev. Lett. **89**, 182501 (2002).
[18] S. C. Pieper and V. R. Pandharipande, Phys. Rev. Lett. **70**, 2541 (1993).
[19] R. B. Wiringa, R. A. Smith, and T. L. Ainsworth, Phys. Rev. C **29**, 1207 (1984).
[20] L. Eisenbud and E. P. Wigner, *Nuclear Structure* (Princeton University Press, Princeton, NJ, 1958).
[21] T. Otsuka, R. Fujimoto, Y. Utsuno, B. A. Brown, M. Honma, and T. Mizusaki, Phys. Rev. Lett. **87**, 082502 (2001).
[22] T. Otsuka, T. Suzuki, R. Fujimoto, H. Grawe, and Y. Akaishi, Phys. Rev. Lett. **95**, 232502 (2005).
[23] J. L. Forest, V. R. Pandharipande, S. C. Pieper, R. B. Wiringa, R. Schiavilla, and A. Arriaga, Phys. Rev. C **54**, 646 (1996).
[24] A. Bohr and B. R. Mottelson, *Nuclear Structure* (Benjamin, New York, 1969), Vol. I, Appendix 1C.
[25] D. R. Tilley, C. M. Cheves, J. L. Godwin, G. M. Hale, H. M. Hofmann, J. H. Kelley, C. G. Sheu, and H. R. Weller, Nucl. Phys. **A708**, 3 (2002).
[26] D. J. Millener, Nucl. Phys. **A693**, 394 (2001).
[27] D. R. Tilley, J. H. Kelley, J. L. Godwin, D. J. Millener, J. E. Purcell, C. G. Sheu, and H. R. Weller, Nucl. Phys. **A745**, 155 (2004).
[28] S. Cohen and D. Kurath, Nucl. Phys. **A101**, 1 (1967).
[29] S. Cohen and D. Kurath, Nucl. Phys. **73**, 1 (1965).
[30] C. J. Horowitz and B. D. Serot, Nucl. Phys. **A368**, 503 (1981).